Determination of limiting factors of photovoltaic efficiency in quantum dot sensitized solar cells: Correlation between cell performance and structural properties

Sixto Giménez,[1] Teresa Lana-Villarreal,[2] Roberto Gómez,[2] Said Agouram,[3,4] V. Muñoz-Sanjosé,[3] and Iván Mora-Seró[1,a)]

[1]*Departament de Física, Photovoltaic and Optoelectronic Devices Group, Universitat Jaume I, 12071 Castelló, Spain*

[2]*Departament de Química-Física i Institut Universitari d'Electroquímica, Universitat d'Alacant, Ap. 99, E-03080 Alacant, Spain*

[3]*Department of Applied Physics and Electromagnetism, University of Valencia, Edif. de Investigación, C/Dr. Moliner 50, 46100 Burjassot, Spain*

[4]*SCSIE, University of Valencia, Edif. de Investigación, C/Dr. Moliner 50, 46100 Burjassot, Spain*

(Received 6 June 2010; accepted 14 July 2010; published online 17 September 2010)

Semiconductor quantum dots (QDs) are important candidates as light absorbing materials in low cost and high efficiency sensitized solar cells (SCs). We present a combination of structural, chemical, electrical, and optical characterization that provides insight to the photovoltaic efficiencies of devices formed by TiO_2 electron conducting oxide network sensitized with CdSe. In devices using colloidal QDs the collection efficiency under short circuit conditions (CESCs) for photoinjected electrons is rather high (~90%) but the photovoltaic performance is limited by the low loading of QDs into the mesoporous TiO_2 structure. On the other hand, chemical bath deposited (CBD) QDSCs exhibit a remarkably high optical density, but only slightly higher short circuit current and efficiency. It is observed that CESC is ~50% due to the high recombination rates of the closed packed QDs structure. Our results indicate routes for improvement of QDSCs performance by the increase in colloidal QDs loading and the reduction in recombination in QDs grown *in situ*.
 [doi:10.1063/1.3477194]

I. INTRODUCTION

Semiconductor nanocrystals (NCs) or quantum dots (QDs) have attracted significant attention in the last years due to the appearance of fascinating physical properties of semiconductors at the nanoscale (when particle size is of the same order than the Bohr exciton radius). Some of these properties are particularly relevant for the development of semiconductor NCs as light absorber elements in solar cell (SC) devices: band gap tunability by size control,[1] intrinsic high extinction coefficients,[1,2] and high dipole moments.[3] At present, there are different QDSC configurations for the exploitation of these properties at the scale of the device.[4] The highest efficiencies have been reported so far employing the QD sensitized nanocrystalline TiO_2 SCs (QDSCs), which have benefited from the optimization advances carried out for dye sensitized (or Gratzel's) SCs (DSC).[5] However, the QDs counterpart of the DSC device is far from being optimized and there is no standard configuration as it is the case of DSCs. In QDSCs issues as the optical absorption,[6] electron injection,[6,7] charge recombination,[8,9] hole scavenging,[10,11] electrolyte,[9,12,13] and series resistance (counterelectrode effect)[14–16] are the subjects of intense study. Close to 2% (Ref. 16) photovoltaic efficiency was recently reported for QDSCs using colloidal CdSe QDs, while higher SC efficiencies, around 3%–4% (Refs. 17 and 18) have been reported for QDSCs using *in situ* deposition methods, under full 1 sun illumination. Consequently, the determination of the limiting factors of SC efficiency is a key factor for QDSCs optimization. The influence of QD preparation and deposition process on the device response also needs to be dealt with. Here we show the main limiting factors for photovoltaic efficiency of QDSCs and propose the directives to overcome these limitations, in order to improve QDSCs performance.

Recently, some new ideas have been introduced to enhance the performance of these devices. These ideas suggest that structural properties of the sensitized electrode play an important role on the final SC performance. Kamat's group has proposed the sequential sensitization of TiO_2 nanostructured electrodes with QDs of different sizes to obtain rainbow SCs.[19] On the other hand, Zaban's group has demonstrated that conformal coating the QD sensitized TiO_2 nanostructure by an amorphous TiO_2 coating allows the use of I^-/I_3^- redox system, leading to increased efficiencies and stability of QDSCs.[13] Additionally, the use of strong dipole molecules adsorbed and/or ZnS coating onto the QDs sensitized TiO_2 nanostructure allows tuning the band alignment of TiO_2 and QDs, also leading to more favorable injection driving force.[20]

In order to correlate the dependence of QDSCs performance with the structural properties of the photoanode, different sensitization methods of the TiO_2 mesoporous network have been analyzed in this work. At present, the main strategies for QD sensitization reported in the literature comprise *in situ* growth methods [chemical bath deposition, CBD

a)Electronic mail: sero@fca.uji.es.

(Refs. 17, 21, and 22) and successive ionic layer adsorption and reaction[12,23–25]] and linking of presynthesized colloidal NCs to the TiO_2 mesoporous structure by means of a bifunctional linker molecule [linker assisted adsorption, LA (Refs. 14 and 26)] or direct adsorption (DA) of colloidal semiconductor NCs to the TiO_2 mesoporous structure by using an adequate solvent in the colloidal solution.[27] In this work, we have correlated the structural characteristics of the QDs sensitized electrodes with the final QDSCs efficiency, identifying the limiting factors for the SC performance. Consequently, the present study is devoted to quantitatively understand both the origin of the differences in photovoltaic efficiency observed for QDSCs, depending on the QD preparation and attaching mode, and the major limiting factors affecting the SC performance, when sensitization is carried out by *in situ* CBD methods or by attaching colloidal QDs by LA or DA. Therefore, a complete structural, chemical, optical, and electrical characterization of photoanodes with QDs deposited by different strategies has been carried out. Based on the obtained results, collection efficiency of photoinjected electrons under short circuit conditions (CESCs) of the devices was estimated and the limiting factors for SC efficiency are discussed.

II. EXPERIMENTAL SECTION

A. Preparation of colloidal CdSe QDs

CdSe QDs, capped with trioctylphosphine (TOP) and dispersed in toluene, were prepared by a solvothermal route that allows size control.[28] Briefly, selenium reacts with cadmium myristate in toluene in the presence of oleic acid and TOP. The reaction takes place at 180 °C in a sealed autoclave for 15 h. The synthesized QDs are characterized by a well-defined peak at 561 nm (first excitonic peak), which reveals a narrow size (diameter) distribution around 3.3 ± 0.1 nm.[1] For DA of QDs onto TiO_2 surface, solvent exchange is needed and a CH_2Cl_2 (99.6%, Sigma Aldrich) CdSe QDs dispersion was prepared by centrifugation of the toluene colloidal dispersion and redissolution.[27] This solution is characterized by a first excitonic peak at 540 nm, also showing a nearly monodisperse size distribution around 2.9 ± 0.1 nm.[1]

B. Preparation of QD sensitized electrodes

A compact layer of TiO_2 (thickness ~100–200 nm) was deposited by spray pyrolisis of titanium(IV) bis(acetoacetonato) di(isopropanoxylate) (Sigma Aldrich) onto the SnO_2:F (FTO) coated glass electrodes (Pilkington TEC15, 15 Ω/sq resistance). The FTO electrodes were kept at 400 °C during spraying to burn off all the organics, thus leaving behind a compact layer of TiO_2. Subsequently, the coated substrate was fired at 450 °C for 30 min. A commercial 20–450 nm particle size TiO_2 paste (18NR-AO, Dyesol, Queanbeyan, Australia) was deposited on top of the TiO_2 compact layer. Around 0.24 cm^2 TiO_2 films were deposited by doctor blade and subsequently sintered at 450 °C for 30 min in a muffle-type furnace. The thickness of the sintered TiO_2 films was approximately 10 μm measured by a profilometer Dektack 6 from Veeco. The TiO_2 photoanodes were sensitized with colloidal QDs following two different strategies: LA (Ref. 14) and DA.[16,27] The dipping time in the QDs solutions was 72 h for both LA and DA strategies. Prior to this step, LA specimens were functionalized by dipping the electrodes into a cysteine solution for 24 h.[14] Additionally, *in situ* growth of QDs on TiO_2 mesoporous films by CBD was also carried out following the procedure published by Gorer and Hodes.[21] First, as the Se source, an 80 mM sodium selenosulphate (Na_2SeSO_3) solution was prepared by dissolving elemental Se powder in a 200 mM Na_2SO_3 solution. Second, 80 mM $CdSO_4$ and 120 mM trisodium salt of nitrilotriacetic acid [$N(CH_2COONa)_3$] were mixed in a volume ratio 1:1. Finally, both solutions were mixed in a volume ratio 1:2. The TiO_2 electrodes were placed in the dark in a glass container filled with the final solution for 12 h deposition time. All the electrodes were coated with ZnS by twice dipping alternately into 0.1 M $Zn(CH_3COO)_2$ and 0.1 M Na_2S solutions for 1 min/dip, rinsing with Milli-Q ultrapure water between dips.[29]

C. SC configuration

The SCs were prepared by assembling an Au counter electrode (prepared by sputtering Au–Pd alloy onto a FTO substrate) and a QDs sensitized FTO/TiO_2 electrode using a silicone spacer (thickness 50 μm) with a droplet (10 μl) of polysulfide electrolyte. It was prepared following the procedure described in Ref. 30: 1 M Na_2S, 1 M S, and 0.1 M NaOH solution in N_2 bubbled Milli-Q ultrapure water.

D. Structural, chemical, optical, and electrical characterization

Microstructural examination of transversal cross-sections of sensitized photoanodes was carried out by a JSM-7000F JEOL FEG-SEM system (Tokio, Japan) equipped with an INCA 400 Oxford EDS analyzer (Oxford, U.K.). Transmission electron microscopy (TEM), high resolution TEM (HRTEM), and energy dispersive x-ray spectroscopy (EDS) was carried out by using a Field Emission Gun (FEG) TECNAI G^2 F20 microscope operated at 200 kV. TEM samples were prepared by raking off the mesoporous sensitized photoanodes from the FTO coated glass. The powder specimens were sonicated in absolute ethanol for 5 min, and a few drops of the resulting suspension were deposited onto a holey-carbon film supported on a copper grid, which was subsequently dried.

The absorption in Kubelka–Munk units of the different TiO_2 electrodes sensitized with QDs has been extracted from their diffuse reflectance using the relation: $F(R)=(1-R)^2/2R$, where R is the measured diffuse reflectance. This representation allows a direct comparison of the amount of QDs adsorbed on each sample. The approximate estimation of the concentration, C, of the QDs adsorbed on the TiO_2 film can be found by the following linear dependence of the Kubelka–Munk function versus C: $F(R)=\varepsilon C/S$, where ε is the extinction coefficient, provided that the scattering coefficient S remains constant for the different TiO_2 films. The diffuse reflectance spectra of QD sensitized TiO_2 samples were recorded by a Varian Cary 500 Scan UV-VIS-NIR spec-

trophotometer with an integration sphere. Current-potential curves were obtained using a FRA equipped PGSTAT-30 from Autolab. The cells were illuminated using a solar simulator at AM 1.5G, where the light intensity was adjusted with a NREL-calibrated Si SC with a KG-5 filter to 1 sun intensity (100 mW cm^{-2}).

The apparent QDs surface coverage of the TiO_2 mesoporous electrodes was estimated by taking into account the electrode real surface area and by measuring the Cd content of each electrode. The CdSe NCs were dissolved in an aqueous 4 wt % H_2O_2 solution containing 3 wt % of HNO_3, prior to chemical analysis by inductively coupled plasma atomic emission spectrometry (Perkin-Elmer Optima 3000). The electrode surface area was determined by a Brunauer-Emmett-Teller (BET) isotherm (Autosorb-6 and Autosorb-Degasser, Quanta chrome), by removing the TiO_2 particles from the as-prepared films after a thermal treatment at 450 °C. Assuming that QDs are monodispersed spheres forming a perfect closed packed hexagonal structure on the TiO_2 surface, the surface coverage of the TiO_2 nanostructure was evaluated for samples using colloidal QDs as sensitizers.[27] Additionally, the theoretical maximum current expected from the photoanodes was calculated by integrating the simulated absorbance curves with the AM 1.5G solar spectrum in the 400–700 nm wavelength interval. The simulated absorbance curves of the photoanodes were obtained by multiplying the absorbance curves of the QDs solution by a factor which takes into account the different concentration of NCs in the solution, obtained at the excitonic peak position,[1] and in the TiO_2 sensitized electrode obtained by the Cd contents.

The absorption spectra of the QDs dispersion have been employed to evaluate the collection efficiency under short circuit conditions (CESC) for the sensitized electrodes on the basis of the amount of CdSe measured by chemical analysis. The maximum expected short circuit current from a 100% conversion of absorbed photons into extracted electrons, I_{max}, has then been calculated. Comparing this value with the short circuit current obtained for the QDSCs, the CESC ratio has been obtained. It should be remarked that the values of CESC are slightly overestimated because the data of optical density for QD in solution have been used for the evaluation. This approximation does not take into account the scattering of the TiO_2 layer and the spectral shift caused by adsorption and ZnS treatment (20–30 nm) but it is appropriated to compare samples analyzed following the same protocol.

III. RESULTS AND DISCUSSION

Figure 1 shows the absorption spectra of the photoanodes after conformal ZnS coating plotted as Kubelka–Munk units. ZnS coating significantly increases the photocurrents in QDSCs (Refs. 9, 16, and 22) due to a reduction in the recombination process of electrons in the TiO_2 with accepting species in the electrolyte.[9] In comparison with noncoated specimens, the presence of the ZnS coating, leads to an slight increase in the absorption peak about 10% and redshifts the spectrum as a consequence of the loss of quantum confinement.[9] The CBD photoanodes are characterized by a much higher optical absorption, four times higher than its DA and LA counterparts, see Fig. 1. Additionally, CBD photoanodes show an absorption plateau at 400–550 nm. In contrast, DA and LA specimens exhibit a clear absorption peak (first excitonic peak) at 563 nm and 590 nm, respectively.

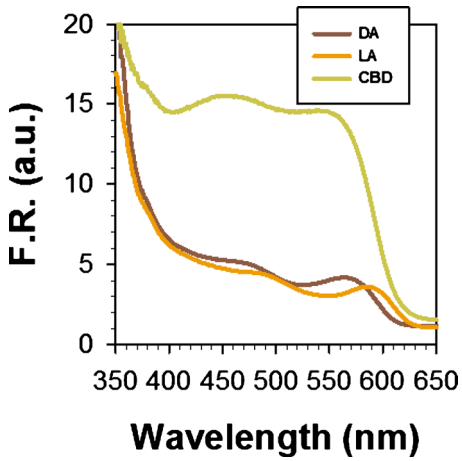

FIG. 1. (Color online) Kubelka–Munk plot of the diffuse reflectance data obtained for TiO_2 mesoporous electrodes sensitized with CBD, LA, and DA NCs after coating with ZnS.

The photovoltaic performance of SC devices fabricated with these sensitized electrodes is showed in Fig. 2 and Table I. The conversion efficiency of the SC devices can be clearly ranked as CBD > DA > LA (1.20%, 1.11%, and 0.85%, respectively) following the same trend as the photocurrent (5.04 mA/cm^2, 4.38 mA/cm^2, and 4.23 mA/cm^2, respectively). The values of V_{oc} are remarkably high, peaking at 0.64 V for DA SCs. It is worth noting that these photovoltaic parameters were obtained two days after assembling the SCs. It has been reported that QDSCs attain their maximum performance some days after cell assembly, probably due to the diffusion and accommodation process of the electrolyte.[12] Comparing QDSC to DSC, the fill factors (FFs) are significantly lower (<0.5 in all cases). This is a consequence of (i) the presence of an aqueous polysulfide electrolyte,[9,31] since the chemical species of water are ideal candidates for recombination centers and (ii) the existence of charge transfer limi-

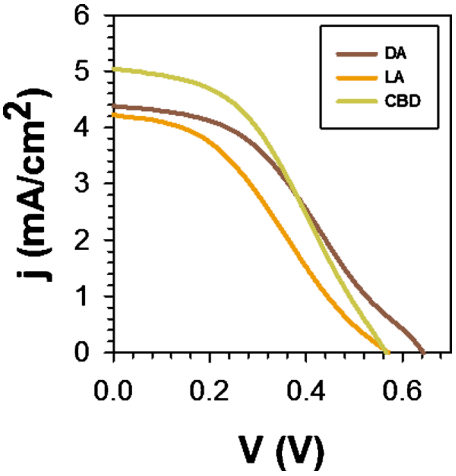

FIG. 2. (Color online) Density-voltage curves of the manufactured QDSCs showing maximum performance for each adsorption strategy.

TABLE I. Photovoltaic properties of QDSCs measured under 1 sun illumination (AM 1.5G). In addition, the table indicates the concentration of QDs in the TiO_2 electrodes: [CdSe] (mg cm^{-2}), d_{QD} (cm^{-2}) and fraction of covered TiO_2 surface, (θ_{QD}) from chemical analysis of the Cd content in each case, and the theoretical maximum current and the CESCs.

Cell	I_{sc} (mA/cm^2)	V_{oc} (V)	FF	η (%)	[CdSe] (mg cm^{-2})	d_{QD} (10^{14} cm^{-2})	θ_{QD}	I_{max} (mA/cm^2)	Estimated CESC (%)
LA	4.23	0.57	0.35	0.85	0.11	3.35	0.200	4.59	88.5
DA	4.38	0.64	0.39	1.11	0.11	4.18	0.221	4.20	99.5
CBD	5.04	0.57	0.42	1.20	0.41	12.8		8.63	55.09

tations between the polysulfide redox electrolyte and conventional platinised counterelectrode.[14,32] These drawbacks have been partially amended by using a Co-redox electrolyte.[23,33] Unfortunately, the slowly diffusing redox species for this Co-redox electrolyte limit the photocurrent of the device. These facts highlight a first limiting factor in QDSCs performance. Consequently, an intense research work is needed in order to find a suitable redox electrolyte, stable, chemically compatible with QD materials and exhibiting low change transfer resistance with conventional counterelectrode materials. On the other hand, QDSCs could also benefit from the current developments in solid state DSCs.[24]

After the electrical characterization of the cells reported in Table I, the SCs were disassembled and the concentration of Cd in the photoanodes was measured by chemical analysis, which provides a precise estimation of the amount of adsorbed QDs. The Cd content values are significantly lower for DA and LA specimens (around 0.1 mg/cm^2) compared to CBD (around 0.4 mg/cm^2), see Table I, in good agreement with optical measurements (Fig. 1). Considering the QDs as spherical and monodispersed features, their surface density, d_{QD}, can be calculated (see Table I). On the basis of a closed packed QD monolayer, the surface area covered by the QDs (A_{QD}) can be worked out. On the other hand, considering the BET specific surface area and the TiO_2 weight of each electrode, it is possible to estimate the total electrode inner surface area (A_{oxide}). The QDs fractional coverage, θ_{QD} would be calculated as A_{QD}/A_{oxide}. A value around 0.2 is obtained for both DA and LA samples, as shown in Table I. This surface coverage is slightly higher compared to that previously reported of ~0.14 using Degusa P25 TiO_2, with particle size between 20 and 80 nm.[27] This is due to the higher mean size of the employed TiO_2 particles, between 20 and 450 nm in this study, indicating that more opened TiO_2 structures favor the incorporation of colloidal NCs to the nanostructured surface. The surface coverage for the CBD specimens cannot be determine in the same way due to: (i) the broad size distribution of NCs in these samples that can be inferred from the absorption plateau observed in the optical absorption measurements, Fig. 1 and (ii) the aggregation observed from TEM images, see below.

In order to ascertain if the SC performance is limited by the amount of QDs absorbing material, CESCs, electron extracted to photon absorbed ratio, has been estimated. The results showed in Table I indicate that QDSCs using colloidal QDs as sensitizers exhibit very high CESC, ~90%, pointing out to a limitation of the cell performance due to a low loading of the absorbing material. This result stresses the fact that QDs loading must be increased in these cells in order to improve their performance. More open nanostructures as nanowires, nanotubes, or inverse opals could be good alternatives to nanoparticle structures in order to improve the characteristics of the TiO_2 matrix. On the other hand, CBD photoanodes show a considerable higher amount of absorbing material but their CESC is remarkably lower compared to LA and DA samples indicating that in this case the photocurrent is not limited by the number of absorbed photons.

In order to gain a further insight into the relationship between structure and photovoltaic performance microscopic evaluation of the sensitized photoanodes was carried out by SEM, TEM and EDS. Figure 3(a) shows a transversal cross section of a mesoporous TiO_2 film on FTO coated glass sensitized with CdSe QDs by CBD. At higher magnification [Fig. 3(b)], the TiO_2 particles can be clearly identified but the CdSe NCs can be only appreciated, even at the maximum resolution of the equipment, by an increase in the roughness of the sensitized electrode. However, the presence of CdSe NCs is straightforward from the compositional profile for Cd and Se [Fig. 3(c)] taken at the dotted line in Fig. 3(a), indicating the homogeneous distribution of CdSe QDs (1:1 stoichiometry) along the TiO_2 film thickness. Similar results were obtained with DA and LA sensitized photoanodes although the measured atomic percentages for Cd and Se were lower.

A more detailed view of the nanostructure of the TiO_2 particles after deposition of the CdSe NCs by the different adsorption strategies was carried out by TEM. Figure 4(a) shows the structure of TiO_2 crystals after DA of CdSe NCs. The selected area electron diffraction [Fig. 4(b)] of the marked zone in Fig. 4(a) clearly illustrates the monocrystalline structure which could be indexed by the Body-centered tetragonal phase (TiO_2 Anatase, space group $I41/amd$ (141) in [111] zone axis (Ref. JCPDS: 2-406). Similar features were observed for LA deposition [Fig. 4(c)]. These micrographs clearly illustrate the low loading of colloidal QDs into the TiO_2 mesoporous structrure for both DA and LA adsorption strategies. The CdSe nanoparticles appear as discrete, uniform crystalline spherical features with diameters around 4 nm at the surface of the TiO_2 anatase phase, explaining the clear excitonic peak observed in the absorption measurements. All CdSe NCs show a well-defined lattice spacing, demonstrating that the nanospheres are highly crystalline with an interplanar spacing of 3.52 Å, corresponding to the (111) lattice spacing of face-centered cubic phase of CdSe, space group $F\text{-}43m$ (216). (Ref. JCPDS: 19-191) [Fig. 4(d)]. Additionally, CdSe QDs possess an amorphous shell, which may account for the organic capping (TOP) employed as

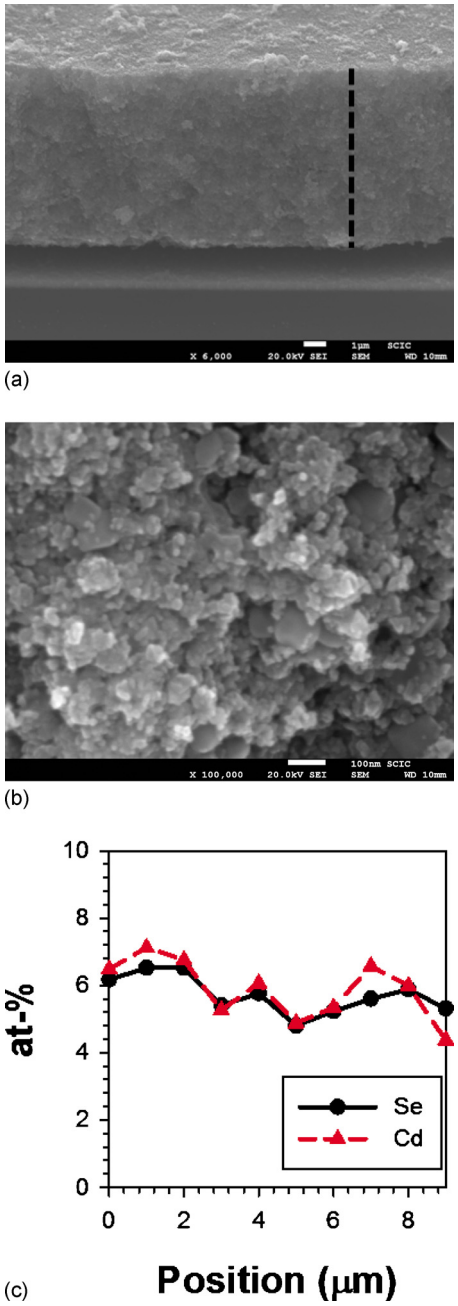

FIG. 3. (Color online) (a) SEM microstructure of the transversal cross section of a FTO/TiO_2 sensitized electrode; (b) closer view of the structure revealing the shape and size of the TiO_2 nanoparticles, and (c) Cd and Se profile (at. %) taken at the dotted line in (a) indicating the homogeneous distribution of CdSe NCs along the film thickness.

surfactant. Indeed, the amorphous shell is extended throughout the surface of the TiO_2 particles as well, as a residue due to the dip-coating process employed to sensitize the TiO_2 mesoporous structure.

A higher load of NCs is observed for CBD sensitized photoanodes [Figs. 4(e) and 4(f)]. In this case, the NCs exhibit a certain degree of aggregation and grain boundaries are clearly observed. From these images, it is clear that the amount of NCs is significantly higher for the CBD specimens compared to DA and LA, which exhibit a low surface covering, in good correspondence with the measured Cd and Se content by EDS showed in Table II. The value reported in

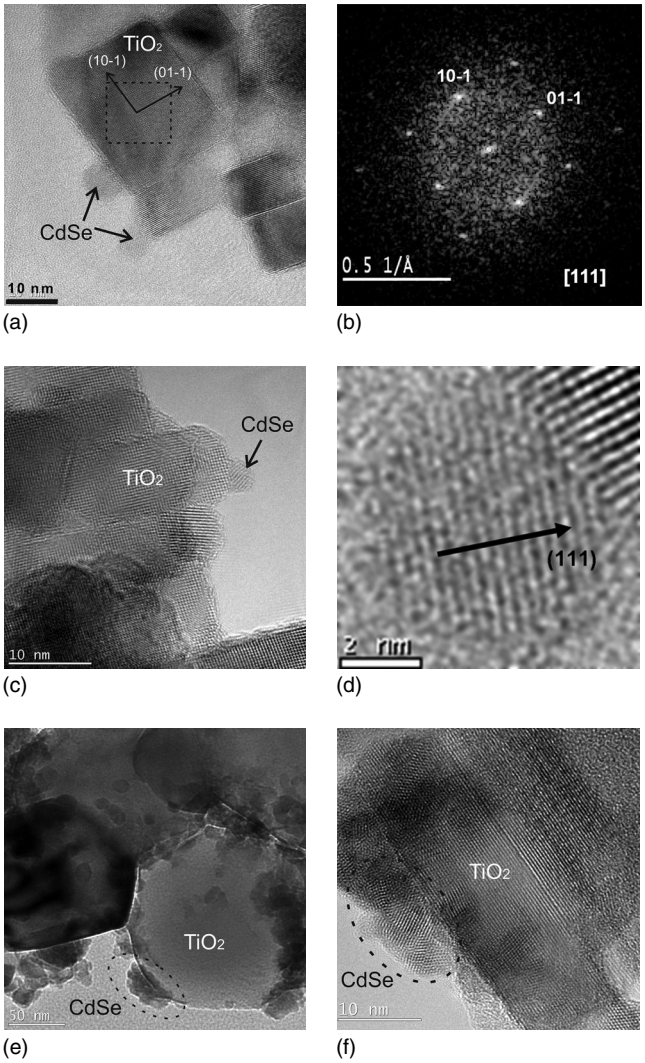

FIG. 4. Bright field TEM images of nanostructured TiO_2 electrodes with QDs deposited by (a) DA, (c) LA, and (e) and (f) CBD. A lower loading of CdSe NCs for DA and LA is evident. (d) HRTEM image of a CdSe colloidal QD illustrating crystalline planes and (b) digital diffractogram pattern of the marked area in (a).

Table II highlights the clear difference in QDs loading between colloidal QDs and CBD sensitized specimens; which has been analyzed by three independent techniques: EDS, optical absorption and chemical analysis, and checked by TEM characterization.

On the other hand, Fig. 5 illustrates the bright field TEM microstructure of the ZnS conformal coating onto a CBD TiO_2/CdSe photoanode. Independently of the deposition strategy for CdSe, ZnS appears as a 2–5 nm thick amorphous layer surrounding both the CdSe NCs and the TiO_2 crystals.

TABLE II. EDS characterization of TEM specimens corresponding to the differently sensitized photoanodes (DA, LA, and CBD).

Cell	Cd (at. %)	Se (at. %)	Ti (at. %)	O (at. %)
LA	0.8	1.1	34.7	63.4
DA	0.7	0.9	32.1	66.3
CBD	3.0	4.1	34.1	58.8

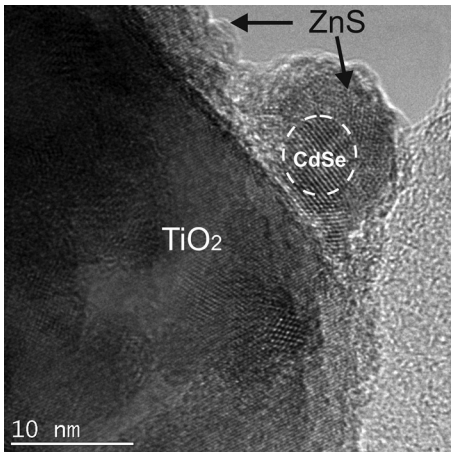

FIG. 5. Illustration of the ZnS conformal coating onto TiO_2/CdSe NC.

This observation satisfactorily explains the role of blocking layer between TiO_2 and the electrolyte previously suggested[9] and responsible for the significant increase in the recombination resistance with the concomitant enhancement of the measured photocurrent as impedance spectroscopy measurements indicates.[9]

The TEM results showed in Figs. 4(e) and 4(f) clearly show that QDs are agglomerated as close packed clusters. Some of the QDs within these clusters are not in direct contact with TiO_2 and grain boundary recombination or electron recombination with the electrolyte before the injection into the TiO_2,[8] can be claimed as the main limiting factors for the CESC obtained for CBD photovoltaic devices. These results are in good agreement with photophysical measurements recently reported using time correlated single photon counting and transient absorption spectroscopy (TAS).[34] TAS measurements show that the recombination kinetics of colloidal QDs electrodes is similar to that reported for DSCs using the N719 dye, while faster recombination kinetics is observed for CBD photoanodes leading to the low CESC values obtained in the present study. The fast internal recombination in CBD clusters limits the QDSCs performance and it should be slowed down in order to improve the performance of these SCs. Fast electron scavenging by coadsorption of metallorganic dyes with QDs has been reported as a promising strategy to slow down this recombination mechanism.[11]

IV. CONCLUSION

Two different limiting factors for the QDSCs performance can be established. One of them arises from the non light absorbing part of the photovoltaic device (electrolyte and counterelectrode), while the other one originates at the light absorbing element (photoanode). The former one points out to the need for developing stable and chemically compatible hole conductor systems. The latter one reflects the key role of the structural properties of the photoanode on the SC performance. From both optical absorption and surface coverage of QDs on the TiO_2 mesoporous structure (characterized by TEM and chemical analysis), it has been shown that the QDs loading is significantly higher for photoanodes with *in situ* grown QDs (CBD) compared to those sensitized by presynthesized QDs (DA and LA counterparts). In spite of this fact, the maximum efficiency of CBD SCs is only slightly higher (10%), since QDSCs using colloidal QDs exhibit a significantly higher CESC. The photovoltaic performance of QDSCs dramatically depends on the preparation and adsorption strategy and it has to be taken into account in the optimization process of these cells. Higher QDs loading (without aggregation) should be achieved in order to increase the performance of photovoltaic devices when colloidal QDs are used as light absorbers. On the other hand, the internal recombination process in CBD QDs clusters should be slowed down in order to increase the photocurrent, and concomitantly, the final efficiency of QDSCs using this sensitizing strategy.

ACKNOWLEDGMENTS

This work was partially supported by the Ministerio de Educación y Ciencia of Spain under the Project Nos. HOPE CSD2007-00007 (Consolider-Ingenio 2010), JES-NANOSOLAR PLE2009-0042, and MAT 2007-66129. S.G. acknowledges the Spanish Ministry of Science and Technology for its financial support through the Ramón y Cajal program. S. Agouram wishes to thank the "Ministerio de Educacion y Ciencia" and the "Fondo Social Europeo" for its financial support. The authors want to acknowledge Professor Juan Bisquert, Dr. Emilio Palomares, Dr. Eugenia Martínez-Ferrero, Dr. Xueqing Xu and Josep Albero for the fruitful discussions on the topics related to this manuscript.

[1] W. Yu, L. H. Qu, W. Z. Guo, and X. G. Peng, Chem. Mater. **15**, 2854 (2003).
[2] P. Wang, S. M. Zakeeruddin, J. E. Moser, R. Humphry-Baker, P. Comte, V. Aranyos, A. Hagfeldt, M. K. Nazeeruddin, and M. Gratzel, Adv. Mater. (Weinheim, Ger.) **16**, 1806 (2004).
[3] R. Vogel, P. Hoyer, and H. Weller, J. Phys. Chem. B **98**, 3183 (1994); R. Vogel, K. Pohl, and H. Weller, Chem. Phys. Lett. **174**, 241 (1990).
[4] A. J. Nozik, Physica E (Amsterdam) **14**, 115 (2002); P. V. Kamat, J. Phys. Chem. C **112**, 18737 (2008).
[5] B. O'Regan and M. Grätzel, Nature (London) **353**, 737 (1991).
[6] I. Mora-Seró, J. Bisquert, Th. Dittrich, A. Belaidi, A. S. Susha, and A. L. Rogach, J. Phys. Chem. C **111**, 14889 (2007).
[7] V. Chakrapani, K. Tvrdy, and P. V. Kamat, J. Am. Chem. Soc. **132**, 1228 (2010); I. Robel, M. Kuno, and P. V. Kamat, *ibid.* **129**, 4136 (2007).
[8] G. Hodes, J. Phys. Chem. C **112**, 17778 (2008).
[9] I. Mora-Seró, S. Giménez, F. Fabregat-Santiago, R. Gómez, Q. Shen, T. Toyoda, and J. Bisquert, Acc. Chem. Res. **42**, 1848 (2009).
[10] I. Mora-Seró, T. Dittrich, A. S. Susha, A. L. Rogach, and J. Bisquert, Thin Solid Films **516**, 6994 (2008).
[11] I. Mora-Seró, D. Gross, T. Mittereder, A. A. Lutich, A. Susha, T. H. Dittrich, A. Belaidi, R. Caballero, F. Langa, J. Bisquert, and A. L. Rogach, Small **6**, 221 (2010).
[12] H. J. Lee, M. Wang, P. Chen, D. R. Gamelin, S. M. Zakeeruddin, M. Grätzel, and M. K. Nazeeruddin, Nano Lett. **9**, 4221 (2009).
[13] M. Shalom, S. Dor, S. Rühle, L. Grinis, and A. Zaban, J. Phys. Chem. C **113**, 3895 (2009).
[14] I. Mora-Seró, S. Giménez, T. Moehl, F. Fabregat-Santiago, T. Lana-Villareal, R. Gómez, and J. Bisquert, Nanotechnology **19**, 424007 (2008).
[15] S.-Q. Fan, B. Fang, J. H. Kim, J.-J. Kim, J.-S. Yu, and J. Ko, Appl. Phys. Lett. **96**, 063501 (2010).
[16] S. Giménez, I. Mora-Seró, L. Macor, N. Guijarro, T. Lana-Villarreal, R. Gómez, L. J. Diguna, Q. Shen, T. Toyoda, and J. Bisquert, Nanotechnology **20**, 295204 (2009).
[17] L. J. Diguna, Q. Shen, J. Kobayashi, and T. Toyoda, Appl. Phys. Lett. **91**, 023116 (2007); O. Niitsoo, S. K. Sarkar, C. Pejoux, S. Rühle, D. Cahen, and G. Hodes, J. Photochem. Photobiol., A **181**, 306 (2006).
[18] Y. L. Lee and Y.-S. Lo, Adv. Funct. Mater. **19**, 604 (2009).

[19]A. Kongkanand, K. Tvrdy, K. Takechi, M. Kuno, and P. V. Kamat, J. Am. Chem. Soc. **130**, 4007 (2008).
[20]E. M. Barea, M. Shalom, S. Giménez, I. Hod, I. Mora-Seró, A. Zaban, and J. Bisquert, J. Am. Chem. Soc. **132**, 6834 (2010); M. Shalom, S. Rühle, I. Hod, S. Yahav, and A. Zaban, *ibid.* **131**, 9876 (2009).
[21]S. Gorer and G. Hodes, J. Phys. Chem. **98**, 5338 (1994).
[22]Q. Shen, J. Kobayashi, L. J. Diguna, and T. Toyoda, J. Appl. Phys. **103**, 084304 (2008).
[23]H. J. Lee, P. Chen, S.-J. Moon, F. Sauvage, K. Sivula, T. Bessho, D. R. Gamelin, P. Comte, S. M. Zakeeruddin, S. I. Seok, M. Grätzel, and M. K. Nazeeruddin, Langmuir **25**, 7602 (2009).
[24]H. J. Lee, H. C. Leventis, S.-J. Moon, P. Chen, S. Ito, S. A. Haque, T. Torres, F. Nüesch, T. Geiger, S. M. Zakeeruddin, M. Grätzel, and M. K. Nazeeruddin, Adv. Funct. Mater. **19**, 2735 (2009).
[25]Y. F. Nicolau, Appl. Surf. Sci. **22–3**, 1061 (1985).
[26]S. K. Leschkies, R. Divakar, J. Basu, E. Enache-Pommer, J. E. Boercker, C. B. Carter, U. R. Kortshagen, D. J. Norris, and E. S. Aydil, Nano Lett. **7**, 1793 (2007); I. Robel, V. Subramanian, M. Kuno, and P. V. Kamat, J. Am. Chem. Soc. **128**, 2385 (2006).
[27]N. Guijarro, T. Lana-Villarreal, I. Mora-Seró, J. Bisquert, and R. Gómez, J. Phys. Chem. C **113**, 4208 (2009).
[28]Q. Wang, D. Pan, S. Jiang, X. Ji, L. An, and B. Jiang, J. Cryst. Growth **286**, 83 (2006).
[29]S. M. Yang, C. H. Huang, J. Zhai, Z. S. Wang, and L. Jiang, J. Mater. Chem. **12**, 1459 (2002).
[30]P. Zhao, H. Zhang, H. Zhou, and B. Yi, Electrochim. Acta **51**, 1091 (2005).
[31]I. Mora-Seró and J. Bisquert, Nano Lett. **3**, 945 (2003).
[32]G. Hodes, J. Manassen, and D. Cahen, J. Electrochem. Soc. **127**, 544 (1980).
[33]H. J. Lee, J.-H. Yum, H. C. Leventis, S. M. Zakeeruddin, S. A. Haque, P. Chen, S. I. Seok, M. Grätzel, and Md. K. Nazeeruddin, J. Phys. Chem. C **112**, 11600 (2008).
[34]E. Martínez-Ferrero, I. Mora-Seró, J. Alberoa, S. Giménez, J. Bisquert, and E. Palomares, Phys. Chem. Chem. Phys. **12**, 2819 (2010).